

# Nonintrusive Uncertainty Quantification of Dynamic Power Systems Subject to Stochastic Excitations

Yiwei Qiu, *Member, IEEE*, Jin Lin, *Member, IEEE*, Xiaoshuang Chen,  
Feng Liu, *Senior Member, IEEE*, and Yonghua Song, *Fellow, IEEE*

**Abstract**—Continuous-time random disturbances (also called stochastic excitations) due to increasing renewable generation have an increasing impact on power system dynamics; However, except from the Monte Carlo simulation, most existing methods for quantifying this impact are *intrusive*, meaning they are not based on commercial simulation software and hence are difficult to use for power utility companies. To fill this gap, this paper proposes an efficient and *nonintrusive* method for quantifying uncertainty in dynamic power systems subject to stochastic excitations. First, the Gaussian or non-Gaussian stochastic excitations are modeled with an Itô process as stochastic differential equations. Then, the Itô process is spectrally represented by independent Gaussian random parameters, which enables the polynomial chaos expansion (PCE) of the system dynamic response to be calculated via an adaptive sparse probabilistic collocation method. Finally, the probability distribution and the high-order moments of the system dynamic response and performance index are accurately and efficiently quantified. The proposed nonintrusive method is based on commercial simulation software such as PSS/E with carefully designed input signals, which ensures ease of use for power utility companies. The proposed method is validated via case studies of IEEE 39-bus and 118-bus test systems.

**Index Terms**—Dynamic uncertainty quantification, Itô process, Karhunen-Loève expansion, polynomial chaos, stochastic differential equations, stochastic excitations

## I. INTRODUCTION

IN recent years, the increasing penetration of renewable generation has posed increasing continuous-time disturbances on power systems. We call these *stochastic excitations* in this paper. The stochastic excitations have a significant impact on system dynamic performance that needs to be quantified to provide information for system operation [1], [2]. Up to now, many works treat renewable generation as static random parameters that do not vary with time, but such simplification may lead to inaccuracy. On the other hand, researches on power system dynamic uncertainty quantification that consider continuous-time stochastic excitations are still in progress.

An adequate method for quantifying the uncertainty of a dynamic power system subject to stochastic excitations should satisfy the following three requirements: 1) *Accuracy*: the result should reflect the probability distribution and high-order moments of the non-Gaussian uncertainty as well as the nonlinearity of the system. 2) *Computational efficiency*: a fast

method enables online evaluation of fast-changing operating conditions. 3) *Ease of use for utility companies*: a nonintrusive method implemented in commercial simulation software is easier to use and more reliable than an intrusive one that uses alternative code to perform a dynamic analysis. Here, *nonintrusive* means that an existing power system simulation tool can be directly employed without rewriting built-in models or numerical solvers; *intrusive* is in contrast to this.

Generally, the Monte Carlo simulation (MCs) is the most straightforward way to power system dynamic uncertainty quantification [2]–[4]. MCs allows precise and nonintrusive assessment of uncertainty, but its inefficiency caused by the large number of samplings hinders its online application.

Emerging methods based on stochastic differential equations (SDEs) [5]–[10] also have drawn significant attention. These methods use SDEs to model dynamic power systems subject to stochastic excitations and then use stochastic calculus to analyze them, and can be traced back to the work of Wang and Crow [9] using the Fokker-Planck equation to describe the evolving probability densities of system states.

However, many of the SDE-based methods rely on the assumption of Gaussian uncertainty [5]–[8], which could be unrealistic in practice; some use partial differential equations, e.g., the Fokker-Planck equation, to depict the evolution of the probability distribution [9], but solving them is computationally expensive; and some use the Feynman-Kac formula to efficiently find the evolving expectation [10] but cannot obtain the probability distribution. In addition, all these methods are *intrusive* because they are not based on commercial simulation software. In these methods, the equations to be solved are derived through highly specialized mathematical knowledge, which have not been included in commercial software to date.

Seen from another perspective, as one of the state-of-the-art methods for uncertainty analysis that considers random parameters, polynomial chaos (PC) [11] has been introduced to power systems. In PC, a series expansion involving Wiener-Askey polynomials is used to represent the impact of random parameters on the system output. It precisely preserves the nonlinear nature of the system and is fast. Applications such as probabilistic power flow [12]–[15], and dynamic uncertainty quantification [16]–[19] have been proposed. Recently, due to community efforts, PC has become increasingly able to handle random parameters. For instance, adaptive sparse techniques have been developed to tackle high-dimensional input [13]–[15], [20], and multi-element PC has been introduced to accommodate evolving probability densities in long-duration dynamic simulations [18], [19].

However, although PC has shown its power in handling

Y. Qiu, J. Lin, X. Chen, and F. Liu are with the State Key Laboratory of Control and Simulation of Power Systems and Generation Equipment, Department of Electrical Engineering, Tsinghua University, Beijing, 100087, China. (email: linjin@tsinghua.edu.cn)

Y. Song is with the Department of Electrical and Computer Engineering, University of Macau, Macau 999078, China, and the Department of Electrical Engineering, Tsinghua University, Beijing 100087, China.

TABLE I  
SUMMARY OF THE FEATURES OF POWER SYSTEM DYNAMIC  
UNCERTAINTY QUANTIFICATION METHODS

| Method                  | Accuracy | Efficiency | Nonintrusive | Continuous<br>Excitations |
|-------------------------|----------|------------|--------------|---------------------------|
| MCs [2]–[4]             | High     | Low        | Yes          | Applicable                |
| SDE-Based [5]–[8], [10] | Fair/Low | High       | No           | Applicable                |
| SDE-Based [9]           | High     | Low        | No           | Applicable                |
| PC-Based [16]–[19]      | High     | High       | Yes          | Inapplicable              |
| Proposed Method         | High     | High       | Yes          | Applicable                |

static random parameters, currently it has trouble dealing with continuous-time stochastic excitations [21]. Karhunen-Loève expansion (KLE) [22], which spectrally decomposes a continuous random process into random parameters, may help PC handle stochastic excitations. Unfortunately, directly combining KLE and PC may result in tremendous complexity [22] and loss of information other than the mean and covariance in describing non-Gaussian uncertainty [23]. For this reason, existing work must assume that the excitations are Gaussian to facilitate the application of PC to their KLEs [20].

To overcome the above discussed drawbacks of the existing methods to achieve decent dynamic uncertainty quantification of power systems subject to stochastic excitations, the following contributions are made in this paper: 1) the dynamic responses of power systems subject to non-Gaussian continuous disturbances are spectrally approximated as functions of discrete Gaussian random parameters based on SDE and KLE, and 2) by applying an adaptive sparse PC-based method to these functions, a method for quantifying the uncertainty in dynamic power systems subject to stochastic excitations that satisfies all three requirements raised above is then proposed.

This paper is organized as follows. Section II introduces the problem of quantifying the power system dynamic uncertainty. Section III presents the Itô process model of stochastic excitations, and the uncertainty quantification method is proposed in Section IV. Finally, in Section V, case studies are used to verify the proposed method.

## II. PROBLEM DESCRIPTION

For a power system subject to continuous-time disturbances, the dynamic response or performance index is a function of the entire *time-domain realization* (or *path*) of the stochastic excitations. Specifically, a power system subject to stochastic excitations can be modeled by a group of differential-algebraic equations with the stochastic excitations  $\xi_t$  as the parameter:

$$dx_t = f(x_t, y_t; \xi_t)dt, \quad (1)$$

$$0 = g(x_t, y_t; \xi_t), \quad (2)$$

where  $x_t$  and  $y_t$  are the state and algebraic variables;  $t$  is time; and  $f(\cdot)$  and  $g(\cdot)$  are the state and algebraic equations.

Without loss of generality, we assume that the solution of (1)–(2) always exists. Then, by fixing the initial state  $x_0$ , the system dynamic response, such as the trajectory of the rotor angle, or performance index, such as CPS1/2 in automatic generation control [10], can be mathematically defined as a function of the entire path of the excitations  $\xi_t$ , denoted by

$$\omega = \omega(\{\xi_\tau\}_{\tau \in [0, t]}), \quad (3)$$

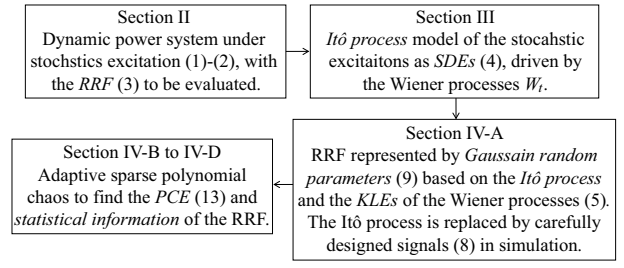


Fig. 1. Brief framework of the proposed method.

where  $\omega(\cdot)$  is referred to as the *random response function* (RRF) in this paper and  $\omega$  represents the value of  $\omega(\cdot)$ .

The goal of quantifying the power system dynamic uncertainty is to extract statistical information on the RRF, such as the expectation and variance, which could help with evaluating the impact of renewable power integration and assessing the security in scheduling and operating the system.

If we replace the continuous excitation in (1)–(2) by static random parameters, then the RRF (3) degrades to a function of the random parameters, and many mature methods, such as those based on polynomial chaos (PC), can be used to evaluate it. Unfortunately, when the excitations are continuous, no existing methods can simultaneously satisfy the three requirements, i.e., accuracy, efficiency, and nonintrusiveness, as noted in the Introduction and summarized in Table I.

To fill this gap, this paper proposes a method for uncertainty quantification of power systems subject to stochastic excitations that satisfies all three of the requirements listed in the Introduction by combining the merits of methods based on SDEs and PC. Briefly, the Gaussian or non-Gaussian stochastic excitations in the power system are modeled with a Itô process, and the RRF is represented by a function of static Gaussian random parameters. Then, the PCE of this function is calculated to extract statistical information about the RRF. The framework of the proposed method is shown in Fig. 1.

## III. MODELING THE STOCHASTIC EXCITATIONS AS SDEs

### A. Modeling Stochastic Excitations Using the Itô Process

Many existing works have shown that the random processes of renewable generation can be represented by the Itô process [2], [10], [24], formulated by the following SDE:

$$d\xi_t = \mu(\xi_t, t)dt + \sigma(\xi_t, t)dW_t, \quad (4)$$

where  $\xi_t$  is the vector of stochastic excitations with dimension  $m$ ;  $W_t = [W_{1,t}, \dots, W_{n,t}]^T$  is the  $n$ -dimensional independent standard Wiener processes (or Brownian motions); and  $\mu(\cdot) : \mathbb{R}^m \times \mathbb{R}_+ \rightarrow \mathbb{R}^m$  and  $\sigma(\cdot) : \mathbb{R}^m \times \mathbb{R}_+ \rightarrow \mathbb{R}^{m \times n}$  are called the *drift* and *diffusion terms*, respectively.

**Remark 1.** With different drift and diffusion terms, Gaussian or non-Gaussian random processes  $\xi_t$  can be depicted by (4).

For example, when the drift term  $\mu(\cdot)$  is affine to  $\xi_t$  and the diffusion term  $\sigma(\cdot)$  is constant,  $\xi_t$  becomes the Ornstein-Uhlenbeck process, which is Gaussian [25] and used in many other works [5]–[8]. Also, using the drift and diffusion terms in Table II, typical Non-Gaussian excitation can be modeled.

The relation between the probability distribution and the drift and diffusion terms is determined by the Fokker-Planck

TABLE II  
DRIFT AND DIFFUSION TERMS OF ONE-DIMENSIONAL ITÔ PROCESSES  
WITH SOME TYPICAL PROBABILITY DISTRIBUTIONS

| Type     | Probability Density                           | $\mu(\xi_t)$                          | $\sigma^2(\xi_t)$             |
|----------|---|---------------------------------------|-------------------------------|
| Gaussian | $e^{(\xi_t - a)^2/2b}/\sqrt{2\pi b}$          | $-(\xi_t - a)$                        | $2b$                          |
| Beta     | $\frac{\xi_t^{a-1}(1-\xi_t)^{b-1}}{B(a,b)}$   | $-\left(\xi_t - \frac{a}{a+b}\right)$ | $\frac{2\xi_t(1-\xi_t)}{a+b}$ |
| Gamma    | $\frac{b^a}{\Gamma(a)}\xi_t^{a-1}e^{-b\xi_t}$ | $-(\xi_t - a/b)$                      | $2\xi_t/b$                    |
| Laplace  | $e^{- \xi_t - a /b}/(2b)$                     | $-(\xi_t - a)$                        | $2b \xi_t - a  + 2b^2$        |

equation [9], [25] (see Appendix A), and the Itô process can be analytically constructed based on the it; see [10] for details.

In addition, we present a data-driven method for identifying the Itô process model from real data; see Appendix B.

### B. Simulation of the Stochastic Excitations

Monte Carlo simulation (MCs) is the most straightforward way to quantify the statistical information in the RRF (3) [2]–[4]. In MCs, paths of the stochastic excitations are sampled via a stochastic numerical integration scheme, for example the Maryuama-Euler (EM) scheme [2], as

$$\xi_{t+h} = h\mu(\xi_t; q) + \sigma(\xi_t; q)\sqrt{h}\zeta, \quad (5)$$

where  $h$  is the step length;  $\zeta \sim \mathcal{N}(0, I)$  is sampled as a vector of independent normal random variables in each step.

Integration scheme (5) implies time-domain discretization of the stochastic excitations is impractical in uncertainty quantification, since the number of the resulting random parameters is proportional to the number of discretization steps, causing the curse of dimensionality. However, discretizing the excitations spectrally instead of in the time domain can be a feasible solution. This is the basic idea of our work, as illustrated later.

## IV. THE UNCERTAINTY QUANTIFICATION METHOD

### A. Spectral Representation of the Stochastic Excitations

According to the Karhunen-Loève theorem [26], a standard Wiener process  $W_{i,t}$  can be orthogonally decomposed into a series of independent standard Gaussian random variables  $\{\zeta_{i,j}\}_{j=1}^\infty$ , known as the *Karhunen-Loève expansion (KLE)*:

$$W_{i,T} = \int_0^T dW_{i,t} = \sum_{j=1}^\infty \zeta_{i,j} \int_0^T m_j(t) dt, \quad (6)$$

where  $\{m_j(t)\}_{j=1}^\infty$  are functions defined on interval  $t \in [0, T]$ :

$$m_j(t) = \begin{cases} \sqrt{1/T} & , j = 1, \\ \sqrt{2/T} \cos[(j-1)\pi t/T] & , j \geq 2. \end{cases} \quad (7)$$

For computation, the infinite series (6) is truncated at a given order  $K$ , which is empirically chosen from between 3 and 6 based on a compromise between precision and computational cost. Taking the derivative of both sides of (6) yields

$$dW_{i,t} \approx \sum_{j=1}^K \zeta_{i,j} m_j(t). \quad (8)$$

Substituting (8) into the Itô process (4) yields the following ordinary differential equation with random coefficients:

$$\frac{d\xi_t^*}{dt}(\zeta) = \mu(\xi_t^*, t) + \sigma(\xi_t^*, t) \sum_{j=1}^K \zeta_j m_j(t), \quad (9)$$

where  $\zeta_j$  is a vector of independent normal random variables with dimension  $n$  and  $\zeta \triangleq \{\zeta_{i,j}\}_{1 \leq i \leq n, 1 \leq j \leq K}$  is the vector of all independent normal random variables. For convenience, in the rest of this paper, we reindex the entries of  $\zeta$  as  $\{\zeta_i\}_{1 \leq i \leq M}$  without ambiguity.  $M = nK$  is the size of  $\zeta$ .

Visual examples of  $\xi_t^*(\zeta)$  as the solution of (9) for fixed values of  $\zeta$  are shown in Fig. 7(b). An intuitive proposition regarding (9) is as follows:

**Proposition 1.** *The solution of (9), i.e.,  $\xi_t^*(\zeta)$ , converges to the Itô process  $\xi_t$  defined in (4) as  $K \rightarrow \infty$ .*

Although this proposition seems straightforward, the rigorous proof is rather arduous. Interested readers are referred to Section 15.5.3 of [26]. With such an approximation, the non-Gaussian stochastic excitations can be characterized by independent Gaussian random variables, which directly facilitates the application of the polynomial chaos based methods.

Finally, by substituting (9) into (3), we find that the system dynamic response or performance index defined by the RRF  $\omega(\cdot)$  can be approximated by an implicit function (denoted by  $\omega^*(\cdot)$ ) of the independent Gaussian random variables, as

$$\omega \approx \omega^*(\zeta) = \omega(\{\xi_\tau^*(\zeta)\}_{\tau \in [0, t]}). \quad (10)$$

Analysis of the convergence of approximation (10) is delayed to the proof of Proposition 2.

This far, we have established the foundation for using Gaussian random parameters to depict the RRF during stochastic excitation as (10), but  $\omega^*(\zeta)$  has still not been expressed explicitly. Fortunately, polynomial chaos provides a way to approximate it explicitly. This is illustrated followingly.

### B. Quantifying Uncertainty Using Polynomial Chaos

Polynomial chaos (PC) uses a series of polynomials orthogonal with respect to the probability density of the random parameters to depict the random outputs [11]. For the standard Gaussian random variables in the KLEs (6) of the Wiener process, the relevant polynomials are the Hermite polynomials,

$$H_n(\zeta_i) = (-1)^n e^{\zeta_i^2/2} \frac{d^n}{d\zeta_i^n} e^{-\zeta_i^2/2}, \quad n \in \mathbb{N}, \quad (11)$$

which admit the following orthogonality:

$$\langle H_j(\cdot), H_k(\cdot) \rangle \triangleq \int_{-\infty}^{+\infty} H_j H_k \frac{e^{-\zeta_i^2/2}}{\sqrt{2\pi}} d\zeta_i = \delta_{jk} \|H_j\|^2, \quad (12)$$

where  $\langle \cdot, \cdot \rangle$  represents an inner product;  $\|\cdot\| = \langle \cdot, \cdot \rangle^{1/2}$  is the 2-norm; and  $\delta_{jk}$  is the Kronecker delta function.

Then, given an order  $N_i$  for each scalar random variable  $\zeta_i$ , the basis  $\{\phi_j(\zeta)\}$  for the random vector  $\zeta$  is constructed as

$$\{\phi_j(\zeta)\} = \{H_{j_1}(\zeta_1) H_{j_2}(\zeta_2) \cdots H_{j_M}(\zeta_M) : j_i \leq N_i\}, \quad (13)$$

where  $j \triangleq [j_1, j_2, \dots, j_M]^T$  is the multi-dimensional index.



Finally, the approximate RRF  $\omega^*(\zeta)$  in (10) can be explicitly approximated by the following polynomial chaos expansion (PCE), which is denoted  $\hat{\omega}(\cdot)$  and formulated as follows:

$$\omega \approx \omega^*(\zeta) \approx \hat{\omega}(\zeta) \equiv \sum_j \hat{c}_j \phi_j(\zeta), \quad (14)$$

where  $\hat{c}_j$  is the coefficient of the PCE. Its exact value is defined by the orthogonal projection  $\hat{c}_j = \langle \omega^*(\zeta), \phi_j(\zeta) \rangle / \|\phi_j(\zeta)\|^2$  [11] but is generally unavailable due to the absence of an explicit expression for  $\omega^*(\zeta)$ .

Instead of rigid orthogonal projection, in practice, either the probabilistic Galerkin method (PGM) or the probabilistic collocation method (PCM) can be used to find the coefficients [11]. Because the PCM is a nonintrusive method whereas the PGM is not, this study uses the PCM to find the coefficients.

### C. PCM for Computing the PCE Coefficients

First, define the set of collocation points (Gaussian quadrature points) that contain all the zeros of the product of the  $(N_i + 1)$ th Hermite polynomials of the random variables in  $\zeta$ :

$$\{\hat{\zeta}_i : H_{N_1+1}(\zeta_1)H_{N_2+1}(\zeta_2) \cdots H_{N_M+1}(\zeta_M) = 0\}_{i=1}^{N_b}, \quad (15)$$

where  $N_b$  is the number of collocation points, which exactly equals the number of basis functions in (13).

For each collocation point  $\hat{\zeta}_i$  in (15), (9) is used to generate the path  $\xi_t^*(\hat{\zeta}_i)$  of excitation  $\xi_t$  as the external input signal, and dynamic simulation software is used to compute the corresponding response,  $\hat{\omega}_i = \omega(\{\xi_\tau^*(\hat{\zeta}_i)\}_{\tau \in [0, t]})$ . Then, the PCE coefficients in (14) can be computed using

$$[\hat{c}_1, \hat{c}_2, \dots, \hat{c}_{N_b}]^T = \mathbf{A}^{-1} [\hat{\omega}_1, \hat{\omega}_2, \dots, \hat{\omega}_{N_b}]^T, \quad (16)$$

where  $\mathbf{A}$  is a constant matrix solely determined by the basis (13) (reindexed as  $\{\phi_i(\cdot)\}_{i=1}^{N_b}$ ) and the collocation points (15):

$$\mathbf{A} = \begin{bmatrix} \phi_1(\hat{\zeta}_1) & \cdots & \phi_{N_b}(\hat{\zeta}_1) \\ \vdots & \ddots & \vdots \\ \phi_1(\hat{\zeta}_{N_b}) & \cdots & \phi_{N_b}(\hat{\zeta}_{N_b}) \end{bmatrix}. \quad (17)$$

Further, since only a few higher-order terms have a noticeable impact on the precision of the PCE [11], we do not need to include all the higher-order terms to construct the PCE.

Alternatively, we use the *Smolyak adaptive sparse algorithm* [27] to incrementally add higher-order terms in an adaptive way until a given error tolerance  $\epsilon$  is reached. The precision of the PCE is assessed by the coefficients. Only the terms with a noticeable impact are added, which markedly decreases the computational cost. Since this algorithm is not a contribution of this paper, to save space, we do not discuss it further. Instead, details of the procedure can be found in [27].

The following proposition lays the mathematical foundation of the proposed method:

**Proposition 2.** *The PCE (14) converges to the RRF (3) as  $K \rightarrow \infty$  and the error tolerance of the Smolyak adaptive sparse collocation method  $\epsilon \rightarrow 0$ .*

*Proof:* From Proposition 1 we know that  $\xi_t^*(\zeta)$  converges to the stochastic excitation  $\xi_t$  as  $K \rightarrow \infty$ . Then, assume the RRF  $\omega(\cdot)$  is bounded with respect to  $\xi_t$ , i.e., there exists a

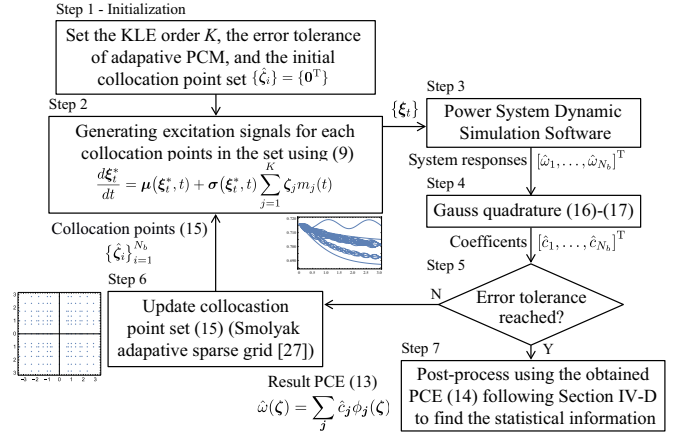


Fig. 2. Flow chart of the proposed uncertainty quantification method.

constant  $L$  such that for any two paths of  $\xi_t$ , say  $\{\xi_\tau^{(1)}\}_{\tau \in [0, t]}$  and  $\{\xi_\tau^{(2)}\}_{\tau \in [0, t]}$ ,  $\|\omega(\{\xi_\tau^{(1)}\}_{\tau \in [0, t]}) - \omega(\{\xi_\tau^{(2)}\}_{\tau \in [0, t]})\| \leq L \|\xi_t^{(1)} - \xi_t^{(2)}\|$  always holds. This assumption is generally true in the operation of power systems unless singularity occurs (see [28]). Thus, combining Proposition 1, we know  $\omega(\zeta)^* \rightarrow \omega(\{\xi_\tau\}_{\tau \in [0, t]})$  as  $K \rightarrow \infty$ , which proves (10).

Finally, the Stone-Weierstrass Theorem implies PCE  $\omega^*(\zeta)$  converges to  $\omega(\zeta)$  as  $N \rightarrow \infty$  [11], and the Smolyak algorithm ensures numerical convergence as its error tolerance  $\epsilon \rightarrow 0$  [27]. Combining the above results concludes the proof. ■

### D. Post-Processing to Extract Statistical Information

From the coefficients in the PCE (14), we can easily find the expectation and variance of the RRF [11] as follows:

$$\mathbb{E}[\omega(\cdot)] = \hat{c}_0, \quad \mathbb{E}[\omega^2(\cdot)] = \sum_j \hat{c}_j^2 \gamma_j, \quad (18)$$

where  $\hat{c}_0$  is the coefficient of the constant basis function in (13) with all  $j_i = 0$  and  $\gamma_j = \|\phi_j(\cdot)\|^2 = j_1! j_2! \cdots j_n!$ .

Additionally, MCs can be used with the PCE (14) to obtain statistical information, e.g., high-order moments. This can be very efficient since the PCE is a simple explicit function and does not require time-domain simulation of the power system.

### E. Overall Computational Procedure

The overall procedure in Fig. 2.

*Step 1:* Set the order  $K$  of the KLE (8), the error tolerance  $\epsilon$  of the Smolyak adaptive sparse algorithm; and initialize the set of collocation points  $\{\hat{\zeta}_i\}$  with only one element  $0^T$ .

*Step 2:* For each point  $\hat{\zeta}$  in the set of collocation points, use (9) to calculate the corresponding excitation signal.

*Step 3:* Use power system simulation software, such as PSS/E, to compute the values of the RRF for each external excitation signal obtained in Step 2.

*Step 4:* Calculate the PCE coefficients based on the PCM, specifically the Gaussian quadrature (16)–(17).

*Step 5:* Based on the change in the coefficients, estimate the approximation error using the method in [27]. If the error tolerance  $\epsilon$  is reached, go to Step 7; otherwise, go to Step 6.

*Step 6:* Update the set of collocation points  $\{\hat{\zeta}_i\}$  based on the changes in the coefficients [27], and return to Step 2.

Step 7: Calculate the statistics using the resulting PCE following Section IV-D, thus concluding the procedure.

## V. CASE STUDIES

### A. Itô Process Modeling of Empirical Stochastic Excitations

We start by demonstrating the ability of the Itô process model (4) to model the uncertainty in renewable, for example wind and solar power generation on different time scales.

1) *Wind Power Uncertainty over Minutes*: Fig. 3 shows the per-unit electrical power generated by an offshore wind farm over a 5-minute interval recorded by Risø DTU at a resolution of 1 point per second [29]. The probability density is shown in Fig. 4(a), and the autocorrelation is shown in Fig. 4(b).

We use quadratic polynomials to construct the drift and diffusion terms. Using the method introduced in the Appendix, the identified Itô process model is formulated as follows:

$$dP_t = [0.0535 - 0.0899P_t + 0.0349P_t^2] dt + [-0.410 + 0.919P_t - 0.505P_t^2] dW_t. \quad (19)$$

A random path of the identified model (19) is simulated and shown in Fig. 3. Visually, the path has a shape of volatility similar to that of the actual curve. Quantitative comparisons of the probability distribution and the autocorrelation are shown in Fig. 4. Clearly, the non-Gaussian distribution and temporal correlation are well characterized.

2) *Solar Power Uncertainty over One Day*: Fig. 5 shows the electrical power generated and injected to the grid by two nearby photovoltaic plants in Sichuan, China on May 30, 2018. Both are normalized by the sine of the solar altitude angle. Their joint probability density is shown in Fig. 6(a).

Based on Fig. 6(a), we assume that there are two correlated beta distributions. Then, the Itô process model is identified as

$$d \begin{bmatrix} P_1 \\ P_2 \end{bmatrix} = \begin{bmatrix} 0.00500 - 0.000280P_1 \\ 0.00513 - 0.000374P_2 \end{bmatrix} dt$$

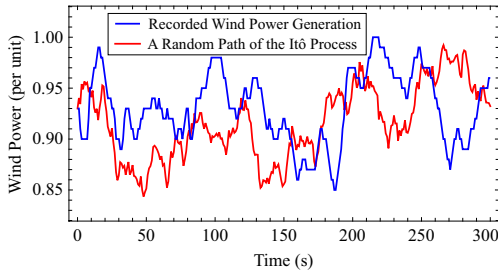


Fig. 3. Power generation of an offshore wind farm over a 5-minute interval recorded by Risø and a random path of the identified Itô process model.

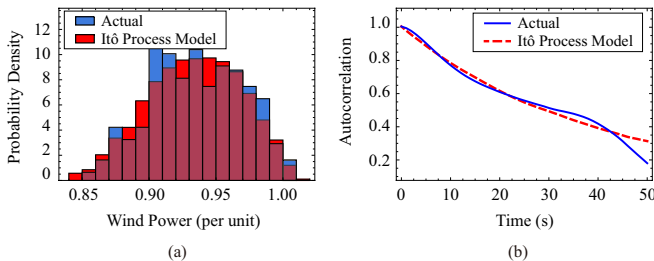


Fig. 4. Probability density and autocorrelation of the actual wind power and the identified Itô process model. (a) Probability density. (b) Autocorrelation.

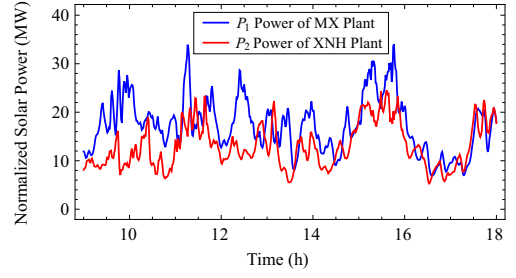


Fig. 5. Solar power output on May 30, 2018 at two pv plants in Sichuan, China. Both are normalized by the sine of the solar altitude angle.

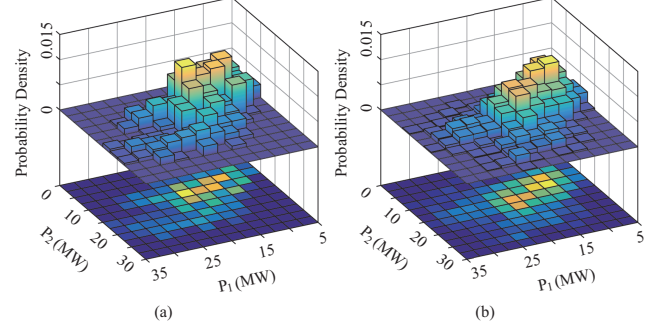


Fig. 6. Joint probability densities of (a) the recorded solar power output, and (b) the simulation of the corresponding Itô process model.

$$+ \begin{bmatrix} 0.00442\sqrt{a} & 0 \\ 0.00271\sqrt{a} & 0.00364\sqrt{b} \end{bmatrix} \begin{bmatrix} dW_{1,t} \\ dW_{2,t} \end{bmatrix}, \quad (20)$$

where  $a = -598.5 + 124.7P_1 - P_1^2$ ;  $b = -404.3 + 85.9P_2 - P_2^2$ . The non-diagonal entries in the diffusion term represent the correlation between the power generated by the two plants.

The simulated joint probability density of the Itô process model is shown in Fig. 6(b). In comparison with Fig. 6(a), the model well depicts the probability distribution and reflects the correlation between the two plants.

### B. IEEE 39-Bus System Case Study

1) *Settings*: The proposed uncertainty quantification method is first tested on the IEEE 39-bus system [30]. The method is implemented in *Python* with dynamic simulation performed by *PSS/E* via *PSSPY* interface. Detailed models of GENROU generators, IEEE1 exciters, and TGOV1 governors are included. A desktop with an Intel i7-8700 CPU is used.

To highlight the ability of the proposed method to handle different types of non-Gaussian uncertainty, three power injections  $P_3, P_{15}$  and  $P_{29}$  with correlated beta and Laplace distributions are connected to buses 3, 15, and 29 to model volatile power generation. Their per-unit values with a base power of 100 MW are modeled by the following Itô process:

$$d \begin{bmatrix} P_3 \\ P_{15} \\ P_{29} \end{bmatrix} = \begin{bmatrix} 0.268 - 0.080P_3 \\ 0.160 - 0.050P_{15} \\ 0.270 - 0.100P_{29} \end{bmatrix} dt + \begin{bmatrix} 0.163\sqrt{c} & 0.1 & 0 \\ -0.082\sqrt{c} & 0.2 & 0 \\ 0 & 0.1 & 0.2\sqrt{d} \end{bmatrix} \begin{bmatrix} dW_{1,t} \\ dW_{2,t} \\ dW_{3,t} \end{bmatrix}, \quad (21)$$

where  $c = -10 + 6.5P_3 - P_3^2$ ;  $d = |2.73 - P_{29}| + 0.01$ . To further demonstrate nonlinearity, a three-phase grounding fault

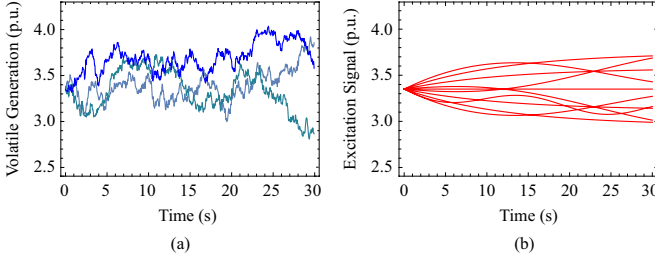


Fig. 7. (a) Three paths of  $P_3(t)$  used in the Monte Carlo simulation. (b) The excitation signals of  $P_3(t)$  used for time-domain simulation in PSS/E with respect to the first 10 collocation points in the proposed method, which have the greatest impact on the precision.

is imposed on bus 3 at  $t = 1$  s and lasts for 0.2 s until it is cleared by tripping line 3-4.

For different orders  $K$  of the KLE and error tolerances  $\epsilon$  of the Smolyak algorithm, with the simulation step length  $h$  set to 0.01 s to generate excitation signals in (5) in the MCs or in (9) in the proposed method, we compare the proposed method to the MCs by finding the probability distribution and high-order moments of the RRF of the post-contingency relative rotor angle  $\delta_{38-30}$  between generators 38 and 30 at  $t = 5$  s and the root-mean-square (RMS) value of the deviation in the system frequency  $\Delta f$  for  $t \in [20, 30]$  s. For visualization purposes, 3 paths of the stochastic excitation  $P_3(t)$  used in the MCs are shown in Fig. 7(a). The signals used for time-domain simulation in PSS/E with respect to the first 10 collocation points in the proposed method, which have the greatest impact on the precision of the PCE, are plotted in Fig. 7(b).

Since obtaining the exact values of the expectation and moments of the RRFs is infeasible for such a complex nonlinear system, we use an MCs with a large enough sampling size  $N_{MC} = 2 \times 10^6$  as a benchmark.

2) *Basic Results:* The probability densities of the relative rotor angle  $\delta_{38-30}$  and the RMS of the frequency deviation  $\Delta f$  computed using the proposed method are compared with the benchmark MCs in Figs. 8 and 9, respectively. As we can

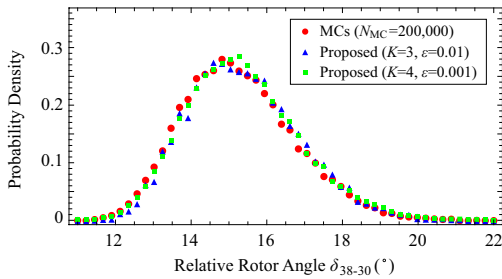


Fig. 8. Probability Density of the relative rotor angles of generators 38 and 30 at  $t = 5$  s obtained by the proposed method and the MCs.

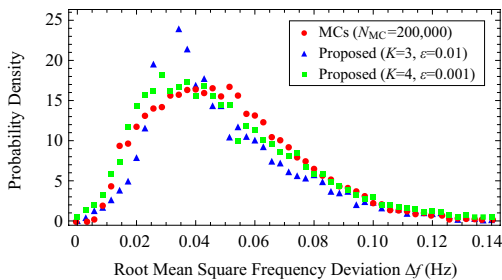


Fig. 9. Probability Density of the root-mean-square deviation of the system frequency for  $t \in [20, 30]$  s obtained by the proposed method and the MCs.

TABLE III  
EXPECTATION, VARIANCE, CENTRAL MOMENTS, AND CORRESPONDING ERROR FOR THE RELATIVE ROTOR ANGLE OBTAINED BY THE PROPOSED METHOD AND THE MCs IN THE 39-BUS SYSTEM CASE

| Method  | Exp.   | Var.   | Central Moment |        |        |
|---|--------|--------|----------------|--------|--------|
|   |        |        | 3rd            | 4th    | 5th    |
| MCs ( $N_{MC} = 2 \times 10^6$ )              | 15.08  | 1.980  | 1.396          | 13.33  | 30.56  |
| MCs ( $N_{MC} = 20,000$ )                     | 15.07  | 1.970  | 1.573          | 13.96  | 35.89  |
|   | -0.07% | -0.51% | +12.7%         | +5.00% | +17.4% |
| MCs ( $N_{MC} = 1,000$ )                      | 15.04  | 1.924  | 1.174          | 11.28  | 19.91  |
|   | -0.28% | -2.83% | -15.9%         | -15.4% | -34.9% |
| Proposed Method ( $K = 3, \epsilon = 0.01$ )  | 15.18  | 1.926  | 1.376          | 12.36  | 26.98  |
|   | +0.64% | -2.73% | -1.43%         | -7.27% | -11.7% |
| Proposed Method ( $K = 3, \epsilon = 0.001$ ) | 15.17  | 1.982  | 1.366          | 13.02  | 28.47  |
|   | +0.62% | +0.10% | -2.15%         | -2.30% | -6.83% |
| Proposed Method ( $K = 4, \epsilon = 0.001$ ) | 15.17  | 2.045  | 1.391          | 13.66  | 29.69  |
|   | +0.61% | +3.28% | -0.36%         | +2.48% | -2.85% |

TABLE IV  
COMPUTATION TIME OF THE PROPOSED METHOD AND THE MCs

| Method  | Time Components (s) |        |                 | Total Time (s) |
|---|---------------------|--------|-----------------|----------------|
|   | Simulation          | Method | Post-Processing |                |
| MCs ( $N_{MC} = 20,000$ )                     | 2207.97             | —      | 0.55            | 2208.52        |
| MCs ( $N_{MC} = 1,000$ )                      | 115.58              | —      | 0.15            | 115.73         |
| Proposed Method ( $K = 3, \epsilon = 0.01$ )  | 9.97                | 0.05   | 1.23            | 11.25          |
| Proposed Method ( $K = 3, \epsilon = 0.001$ ) | 37.85               | 0.17   | 3.03            | 41.05          |
| Proposed Method ( $K = 4, \epsilon = 0.001$ ) | 55.87               | 0.26   | 4.88            | 61.01          |

see, for the relative rotor angle  $\delta_{38-30}$ , the proposed method produces results that are almost identical to those of the benchmark MCs with different settings of  $K$  and  $\epsilon$ . For the RMS of the frequency deviation  $\Delta f$ , the result of the proposed method is not very accurate when  $K = 3$  and  $\epsilon = 0.01$ ; when  $K$  is increased to 4 and  $\epsilon$  is decreased to 0.001, the obtained PDF converges to the actual one. In other words, the RRFs can be precisely extracted using the proposed method.

Furthermore, a quantitative comparison is made in Table III by comparing the expectation and central moments of the relative angle  $\delta_{38-30}$  obtained by the proposed method and the MCs with different settings. The relative error compared to the benchmark MCs is also listed. The numerical results in Table III show that the MCs with  $N_{MC} = 1,000$  or 20,000 both leads to a significant error. In contrast, the proposed method has a much better accuracy with different settings.

The computation time is also compared in Table IV, where the simulation component indicates the time required for dynamic simulation in PSS/E, the method component indicates the time required for the Gaussian quadrature (16)–(17) and the procedure control, and the post-processing component represents the time required for the extraction of statistical information using the MCs based on the PCE.

Obviously the proposed method requires significantly less time than MCs to achieve comparable precision. This is because the key information of the uncertainty is already present in the carefully constructed excitation signals (9) shown in Fig. 7(b). Therefore, a few simulations suffice to extract most of the statistical information. In fact, with  $K = 3$  and  $\epsilon = 0.01$ , only 83 simulations are needed instead of the tens of thousands required by the MCs to achieve comparable precision.

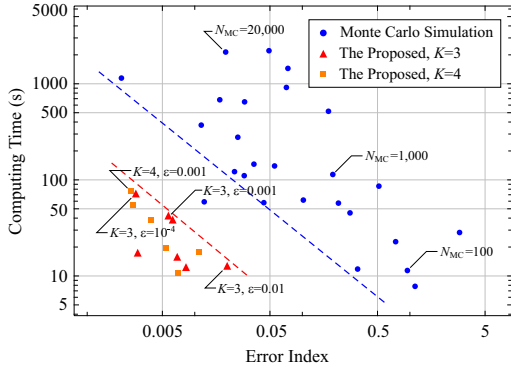


Fig. 10. Computation time versus error index for the proposed method and the Monte Carlo simulation with different settings for the 39-bus system.

3) *Comprehensive Comparison*: Since both the proposed method and the MCs have adjustable precision settings, i.e.,  $K$  and  $\epsilon$  in the proposed method and  $N_{MC}$  in the MCs, to compromise between precision and the computational burden, we repeatedly apply them with different settings to make a comprehensive comparison. To quantify the precision, we define an error index as the sum of the squares of the relative errors of the expectation and the first 5 central moments, as:

$$err = \left[ (E - \hat{E})/E \right]^2 + \sum_{j=2}^5 \left[ (M^{(j)} - \hat{M}^{(j)})/M^{(j)} \right]^2 \quad (22)$$

where  $E$  and  $\hat{E}$  represent the benchmark and obtained expectation of the RRF;  $M^{(j)}$  and  $\hat{M}^{(j)}$  represent those of the  $j$ th central moment.

Fig. 10 shows the computation time versus the precision of the proposed method and the MCs in logarithmic coordinates. Although both methods exhibit negative correlations between the error index and the computation time, the results of the proposed method are more than one to two orders of magnitude better than those of the MCs. Moreover, the results of the MCs vary over a very wide range for a given setting, which is inherent in the nature of random sampling. In contrast, the proposed method performs much more consistently, as only deterministic simulations are required to find the PCE.

4) *Case of Instability*: The proposed method is also tested when instability occurs. To induce instability, a three-phase grounding fault is imposed on bus 39 at  $t = 1$  s and lasts for 0.2 s until it is cleared by tripping line 39-9. Other settings are the same as the previous case. The post-fault relative rotor angle between generators 39 and 30, i.e.,  $\delta_{39-30}$ , is investigated.

For easy understanding, we plot 100 random trajectories of  $\delta_{39-30}(t)$  for  $t \in [0, 5]$  s. The proposed method with  $K = 3$  and  $\epsilon = 0.01$  is used to find the probability density of  $\delta_{39-30}$  at  $t = 2.6$  s and 5 s, respectively. The results compared to the MCs are plotted in Figs. 12.

For  $t = 2.6$  s, the proposed method precisely captures the probability density of the divergent rotor angle, where only 153 simulations are performed. The first 3 orders of moments obtained are 1172.7,  $1.389 \times 10^6$ , and  $1.660 \times 10^9$ , which are almost identical to the results of 1171.8,  $1.383 \times 10^6$ , and  $1.646 \times 10^9$  obtained by MCs with  $N_{MC} = 2 \times 10^6$ .

As of  $t = 5$  s, from Fig. 12(b), the probability distribution become almost discrete, and the density looks like two im-

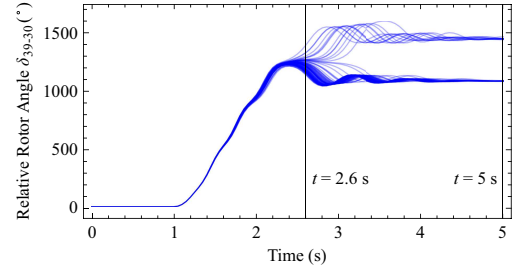


Fig. 11. 100 random trajectories of the relative rotor angle between generators 39 and 30 for  $t \in [0, 5]$  s when instability occurs.

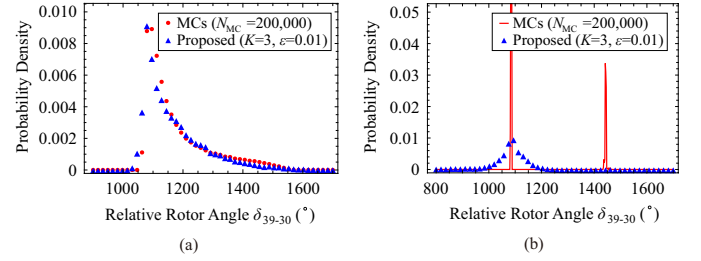


Fig. 12. Probability Density of the relative rotor angles of generators 39 and 30 obtained by the proposed method and MCs. (a)  $t = 2.6$  s. (b)  $t = 5$  s.

pulses. Obviously, it is difficult to use a PCE of normal random variables to approximate such a distribution. Investigating the method for this case can be an interesting future work.

### C. IEEE 118-Bus System Case Study

1) *Settings*: To further verify the proposed method in larger systems with high-dimensional stochastic excitation inputs, we test it on the IEEE 118-bus system [31]. Fifteen stochastic excitations defined by 5 independent sets of (21) are connected as power injections to buses 54, 59, 80, 7, 14, 117, 19, 31, 46, 47, 49, 70, 44, 51, and 97, as shown in Fig. 13. A three-phase grounding is applied to bus 49 at  $t = 1$  s and lasts for 0.2 s until it is cleared by tripping line 49-69. The uncertainty in the relative rotor angle  $\delta_{69-49}$  between generators 69 and 49 at  $t = 5$  s is quantified.

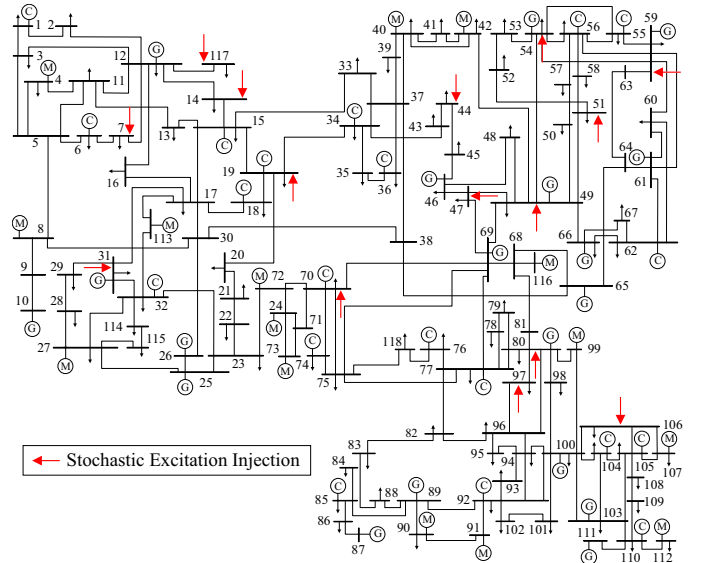


Fig. 13. Diagram of the 118-bus system. The injection points of the 15 stochastic excitations are labeled.



TABLE V  
COMPUTATION TIME OF THE PROPOSED METHOD AND THE MCS IN THE  
IEEE 118-BUS SYSTEM CASE

| Method  | Time Components (s) |        |                 | Total Time (s) |
|---|---------------------|--------|-----------------|----------------|
|   | Simulation          | Method | Post-Processing |                |
| MCs ( $N_{MC} = 20,000$ )                       | 6113.0              | —      | 0.5             | 6113.6         |
| MCs ( $N_{MC} = 2,000$ )                        | 596.9               | —      | 0.2             | 597.1          |
| Proposed Method<br>( $K = 3, \epsilon = 0.01$ ) | 285.2               | 1.1    | 7.5             | 293.8          |

TABLE VI  
EXPECTATION, VARIANCE, CENTRAL MOMENTS, AND CORRESPONDING  
ERROR FOR THE RELATIVE ROTOR ANGLE OBTAINED BY THE PROPOSED  
METHOD AND THE MCS IN THE 118-BUS SYSTEM CASE

| Method  | Exp.   | Var.   | Central Moment |         |         |
|---|--------|--------|----------------|---------|---------|
|   |        |        | 3rd            | 4th     | 5th     |
| MCs ( $N_{MC} = 2 \times 10^6$ )                | 17.24  | 0.749  | -0.137         | 1.700   | -1.012  |
| MCs ( $N_{MC} = 20,000$ )                       | 17.22  | 0.740  | -0.176         | 1.727   | -1.157  |
|   | -0.10% | -1.12% | +7.50%         | +1.60%  | +14.35% |
| MCs ( $N_{MC} = 2,000$ )                        | 17.23  | 0.775  | -0.180         | 1.950   | -1.341  |
|   | +0.04% | +3.46% | +31.42%        | +14.72% | +32.54% |
| Proposed Method<br>( $K = 3, \epsilon = 0.01$ ) | 17.20  | 0.726  | -0.134         | 1.631   | -1.033  |
|   | -0.22% | -2.96% | -1.68%         | -4.06%  | +2.10%  |

2) *Basic Results:* Let  $K = 3$  and  $\epsilon = 0.01$ , the proposed method takes 293.8 s to find the expectation and moments of  $\delta_{69-49}$ . In the proposed method, 941 simulations are performed on PSS/E to evaluate the collocation points. Meanwhile, the MCs with  $N_{MC} = 2,000$  takes 597.1 s, and the MCs with  $N_{MC} = 20,000$  takes 6113.6 s, as listed in Table V. Moreover, using result of the MCs with  $N_{MC} = 2 \times 10^6$  as a benchmark, the error index defined by (22) for the proposed method is  $3.26 \times 10^{-3}$ , which is substantially better than the value of 0.227 for the MCs with  $N_{MC} = 2,000$ , and is also much better than the value of  $2.66 \times 10^{-2}$  for the the MCs with  $N_{MC} = 20,000$ . Detailed comparison of the calculated statistical information is given in Table VI. Obviously, the proposed method significantly outperforms the MCs in this larger power system with higher-dimensional stochastic inputs.

3) *Discussions on Computation Cost versus the Dimension of Stochastic Excitation Inputs:* Finally, we investigate the relation between the computation time consumed by the proposed method and the dimension of the stochastic excitations. With the dimension ranging between 3 and 15, the computation time is shown in Table VII. We can see that the computation time of the proposed method is almost linear with respect to the dimension of random inputs, which means the proposed method is able to handle tens of random inputs. However, as the inherent limitation of a PCE-based method [14], [15], the proposed method cannot accommodate very large number of random inputs. To deal with this situation, it could be possible to use dimension reduction techniques to reduce the number of independent random driving forces of the excitations (the standard Wiener processes  $W_t$  in this case), which may further improve the efficiency of the proposed method.

## VI. CONCLUSIONS

A nonintrusive method for quantifying the uncertainty in dynamic power systems based on SDE and PCE is proposed in this paper. The proposed method exhibits high precision and efficiency compared to the Monte Carlo simulation. The

TABLE VII  
COMPUTATION TIME OF THE PROPOSED METHOD WITH DIFFERENT  
DIMENSION OF STOCHASTIC EXCITATIONS IN THE IEEE 118-BUS  
SYSTEM CASE

| Random Inputs | Time Components (s) |        |                 | Total Time (s) |
|---------------|---------------------|--------|-----------------|----------------|
|               | Simulation          | Method | Post-Processing |                |
| 3             | 22.9                | 0.1    | 1.3             | 24.3           |
| 6             | 71.2                | 0.2    | 2.8             | 74.1           |
| 9             | 138.1               | 0.6    | 4.3             | 143.0          |
| 12            | 199.7               | 0.8    | 4.8             | 205.4          |
| 15            | 285.2               | 1.1    | 7.5             | 293.8          |

method runs on commercial simulation software such as PSS/E, which ensures ease of use for power utilities.

Extending the proposed method from the Itô process driven by Wiener processes relevant to Hermite PC to other random processes related to the generalized polynomial chaos (gPC) to handle more complicated stochastic phenomena in power systems is one of the promising directions for future research.

## APPENDIX A THE FOKKER-PLANCK EQUATION

The probability density of the Itô process evolving with time admits the following partial differential equation, known as the *Fokker-Planck equation*, formulated as

$$\frac{\partial p(\xi_t, t)}{\partial t} = - \sum_{j=1}^m \frac{\partial}{\partial \xi_j} [\mu_j(\xi_t, t) p(\xi_t, t)] + \sum_{j=1}^m \sum_{k=1}^m \frac{\partial^2}{\partial \xi_j \partial \xi_k} [D_{jk}(\xi_t, t) p(\xi_t, t)], \quad (A1)$$

where  $p(\cdot)$  is the probability density function (PDF) of  $\xi_t$ ;  $\xi_j$  is the  $j$ th entry of  $\xi_t$ ;  $D(\cdot) = \sigma(\cdot)\sigma^T(\cdot)/2$ ; and  $D_{jk}(\cdot)$  is the  $k$ th entry in the  $j$ th row of  $D(\cdot)$ . By setting the left-hand side to zero, the stationary state is represented.

## APPENDIX B METHOD FOR IDENTIFYING THE ITÔ PROCESS MODEL

Suppose a set of recorded data of renewable generations with sampling interval  $h$ , denoted by  $\{\tilde{\xi}_0, \tilde{\xi}_h, \tilde{\xi}_{2h}, \dots, \tilde{\xi}_T\}$ . Construct the drift and diffusion terms  $\mu(\xi_t; q)$  and  $\sigma(\xi_t; q)$  in (4) as simple functions of  $\xi_t$ , such as polynomials with parameters  $q$  to be identified, such that the likelihood of the following logarithmic conditional probability is maximized:

$$\max_q L = \log \Pr [\tilde{\xi}_h, \tilde{\xi}_{2h}, \dots, \tilde{\xi}_T | \tilde{\xi}_0]. \quad (B1)$$

By the independent incremental property of the Itô process [25], the conditional probability in (B1) can be rewritten as

$$L = - \sum_{j=1}^{T/h} \log \Pr [\tilde{\xi}_{jh} | \tilde{\xi}_{(j-1)h}]. \quad (B2)$$

Considering the discrete form (5) of the Itô process (4), and considering that the sampling interval  $h$  is short, we obtain

$$\xi_{t+h} \sim \mathcal{N}(\xi_t + h\mu(\xi_t; q), h\sigma^T(\xi_t; q)\sigma(\xi_t; q)). \quad (B3)$$



Therefore, the conditional probability in (B2) is

$$\Pr[\tilde{\xi}_{t+h}|\tilde{\xi}_t] = \frac{1}{\sqrt{(2\pi h)^m \det(\tilde{\sigma}_t \tilde{\sigma}_t^T)}} \times \exp \left\{ -\frac{1}{2} [\Delta\tilde{\xi}_t - h\tilde{\mu}_t]^T (\tilde{\sigma}_t \tilde{\sigma}_t^T)^{-1} [\Delta\tilde{\xi}_t - h\tilde{\mu}_t] \right\}, \quad (\text{B4})$$

where  $\Delta\tilde{\xi}_t = \tilde{\xi}_{t+h} - \tilde{\xi}_t$  represents the change in the recorded data over a sampling interval;  $\tilde{\mu}_t$  and  $\tilde{\sigma}_t$  represent  $\mu(\tilde{\xi}_t; q)$  and  $\sigma(\tilde{\xi}_t; q)$ , respectively.

Substituting (B4) into (B2), letting  $\tilde{D}_{jh} = h\tilde{\sigma}_{jh}\tilde{\sigma}_{jh}^T/2$ , and neglecting the constant terms in the logarithmic function yields

$$\min_q L' = \frac{1}{4} \sum_j [\Delta\tilde{\xi}_{jh} - h\tilde{\mu}_{jh}]^T \tilde{D}_{jh}^{-1} [\Delta\tilde{\xi}_{jh} - h\tilde{\mu}_{jh}] + \frac{1}{2} \sum_j \log \det(\tilde{D}_{jh}). \quad (\text{B5})$$

Model (B5) is a typical unconstrained programming. Hence, common methods such as the gradient descent can be used to find the optimal parameters for the Itô process model.

## REFERENCES

- [1] X. Wang, H.-D. Chiang, J. Wang, H. Liu, and T. Wang, "Long-term stability analysis of power systems with wind power based on stochastic differential equations: Model development and foundations," *IEEE Trans. Sust. Energy*, vol. 6, no. 4, pp. 1534–1542, Oct. 2015.
- [2] F. Milano and R. Zárate-Miñano, "A systematic method to model power systems as stochastic differential algebraic equations," *IEEE Trans. Power Syst.*, vol. 28, no. 4, pp. 4537–4544, Nov. 2013.
- [3] Z. Y. Dong, J. H. Zhao, and D. J. Hill, "Numerical simulation for stochastic transient stability assessment," *IEEE Trans. Power Syst.*, vol. 27, no. 4, pp. 1741–1749, Nov. 2012.
- [4] A. Ortega and F. Milano, "Stochastic transient stability analysis of transmission systems with inclusion of energy storage devices," *IEEE Trans. Power Syst.*, vol. 33, no. 1, pp. 1077–1079, Jan. 2018.
- [5] D. Apostolopoulou, A. D. Domínguez-Garc, and P. W. Sauer, "An assessment of the impact of uncertainty on automatic generation control systems," *IEEE Trans. Power Syst.*, vol. 31, no. 4, pp. 2657–2665, 2016.
- [6] P. Ju, H. Li, C. Gan, Y. Liu, Y. Yu, and Y. Liu, "Analytical assessment for transient stability under stochastic continuous disturbances," *IEEE Trans. Power Syst.*, vol. 33, no. 2, pp. 2004–2014, Mar. 2018.
- [7] Q. Shi, Y. Xu, Y. Sun, W. Feng, F. Li, and K. Sun, "Analytical approach to estimating the probability of transient stability under stochastic disturbances," in *2018 IEEE PESGM*, Portland, USA, 2018, pp. 1–5.
- [8] H. Li, P. Ju, C. Gan, S. You, F. Wu, and Y. Liu, "Analytic analysis for dynamic system frequency in power systems under uncertain variability," *IEEE Trans. Power Syst.*, vol. 34, no. 2, pp. 982–993, Mar. 2019.
- [9] K. Wang and M. L. Crow, "The Fokker-Planck equation for power system stability probability density function evolution," *IEEE Trans. Power Syst.*, vol. 28, no. 3, pp. 2994–3001, Aug. 2013.
- [10] X. Chen, J. Lin, F. Liu, and Y. Song, "Stochastic assessment of AGC systems under non-Gaussian uncertainty," *IEEE Trans. Power Syst.*, vol. 34, no. 1, pp. 705–717, Jan. 2019.
- [11] D. Xiu, *Numerical Methods for Stochastic Computations: A Spectral Method Approach*. Princeton University Press, 2010.
- [12] H. Wu, Y. Zhou, S. Dong, and Y. Song, "Probabilistic load flow based on generalized polynomial chaos," *IEEE Trans. Power Syst.*, vol. 32, no. 1, pp. 820–821, Jan. 2017.
- [13] F. Ni, P. H. Nguyen, and J. F. G. Cobben, "Basis-adaptive sparse polynomial chaos expansion for probabilistic power flow," *IEEE Trans. Power Syst.*, vol. 32, no. 1, pp. 694–704, Jul. 2017.
- [14] X. Sun, Q. Tu, J. Chen, C. Zhang, and X. Duan, "Probabilistic load flow calculation based on sparse polynomial chaos expansion," *IET Generat. Transm. & Distrib.*, vol. 12, no. 11, pp. 2735–2744, Jun. 2018.
- [15] Y. Xu, L. Mili, and J. Zhao, "Probabilistic power flow calculation and variance analysis based on hierarchical adaptive polynomial chaos-ANOVA method," *IEEE Trans. Power Syst.*, vol. 34, no. 5, pp. 3316–3325, Sep. 2019.
- [16] J. R. Hockenberry and B. C. Lesieutre, "Evaluation of uncertainty in dynamic simulations of power system models: The probabilistic collocation method," *IEEE Trans. Power Syst.*, vol. 19, no. 3, pp. 1483–1491, Aug. 2004.
- [17] L. Li, Y. Qiu, H. Wu, Y. Song, and L. Xiao, "Uncertainty analysis of power system time-domain simulation based on generalized polynomial chaos method," in *2017 IEEE PESGM*, Chicago, USA.
- [18] P. Prempraneerach, F. S. Hover, M. S. Triantafyllou, and G. E. Karniadakis, "Uncertainty quantification in simulations of power systems: Multi-element polynomial chaos methods," *Rel. Eng. & Syst. Safety*, vol. 95, no. 6, pp. 632–646, Jun. 2010.
- [19] Y. Xu, L. Mili, A. Sandu, J. Zhao, and M. R. V. Spakovs, "Propagating uncertainty in power system dynamic simulations using polynomial chaos," *IEEE Trans. Power Syst.*, vol. 34, no. 1, pp. 338–348, Jan. 2019.
- [20] J. Li, N. Ou, G. Lin, and W. Wei, "Compressive sensing based stochastic economic dispatch with high penetration renewables," *IEEE Trans. Power Syst.*, vol. 34, no. 2, pp. 1438–1449, Mar. 2019.
- [21] B. J. Debuschere, H. N. Najm, P. P. Pébay, O. M. Knio, R. G. Ghanem, and O. P. Le Maître, "Numerical challenges in the use of polynomial chaos representations for stochastic processes," *SIAM J. Sci. Comput.*, vol. 26, no. 2, pp. 698–719, 2004.
- [22] S. Park, M. Williams, A. K. Prinja, and M. D. Eaton, "Modelling non-Gaussian uncertainties and the Karhunen-Loève expansion within the context of polynomial chaos," *A. Nucl. Energy*, vol. 76, pp. 146–165, Feb. 2015.
- [23] M. Williams, "Polynomial chaos functions and stochastic differential equations," *A. Nucl. Energy*, vol. 33, no. 9, pp. 774–785, Jun. 2006.
- [24] H. Verdejo, A. Awerkin, E. Saavedra, W. Kliemann, and L. Vargas, "Stochastic modeling to represent wind power generation and demand in electric power system based on real data," *Appl. Energy*, vol. 173, pp. 283–295, Jul. 2016.
- [25] E. Pardoux and A. Răşcanu, *Stochastic Differential Equations, Backward SDEs, Partial Differential Equations*. Springer, 2014.
- [26] P. K. Friz and N. B. Victoir, *Multidimensional stochastic processes as rough paths: theory and applications*. Cambridge University Press, 2010.
- [27] P. R. Conrad and Y. M. Marzouk, "Adaptive Smolyak pseudospectral approximations," *SIAM J. Sci. Comput.*, vol. 35, no. 6, pp. A2643–A2670, Nov. 2013.
- [28] K. Wang and M. L. Crow, "Investigation on singularity of stochastic differential algebraic power system model," in *2011 North American Power Symposium*, Boston, MA, USA, Sep. 2011, pp. 1–5.
- [29] J. Lin, Y. Sun, L. Cheng, and W. Gao, "Assessment of the power reduction of wind farms under extreme wind condition by a high resolution simulation model," *Appl. Energy*, vol. 96, pp. 21–32, 2012.
- [30] Illinois Center for a Smarter Electric Grid (ICSEG). (2019, Oct.) IEEE 39-bus system. [Online]. Available: <http://icseg.iti.illinois.edu/ieee-39-bus-system/>
- [31] KIOS Center for Intelligent Systems & Networks, University of Cyprus. (2019, Oct.) IEEE 118-bus modified test system. [Online]. Available: <http://www.kios.ucy.ac.cy/testsystems/index.php/dynamic-ieee-test-systems/ieee-118-bus-modified-test-system>